CMS Physics Analysis Summary

Contact: cms-pag-conveners-heavyions@cern.ch 2017/02/07

Measurement of Nuclear Modification Factors of Y(nS) Mesons in PbPb Collisions at $\sqrt{s_{\mathrm{NN}}} = 5.02$ TeV

The CMS Collaboration

Abstract

The cross sections of Y(1S), Y(2S), and Y(3S) production in PbPb and pp collisions at $\sqrt{s_{\mathrm{NN}}} = 5.02$ TeV are reported. The nuclear modification factors, R_{AA}, derived from the PbPb-to-pp ratio of yields for each state, are studied as a function of rapidity, transverse momentum and centrality. A strong modification is observed for all Y states. The suppression of Y(1S) seen in PbPb collisions at $\sqrt{s_{\mathrm{NN}}}$ = 5.02 TeV is stronger than the previous one measured at $\sqrt{s_{\mathrm{NN}}} = 2.76$ TeV, consistent with an increase in the medium temperature at the higher energy. We obtain an upper limit on the production of Y(3S) of 0.071 at 95% confidence level, the smallest value measured for a hadron R_{AA} in heavy ion collisions so far.

1 Introduction

The measurement of quarkonia in heavy ion collisions is one of the most promising ways of studying the properties of strongly interacting matter at large energy density and high temperature. It was suggested that a strongly interacting medium of deconfined quarks and gluons is produced in this environment, which is often referred to as quark-gluon plasma (QGP) [1, 2]. The bottomonium states are produced during the early stage of collision via hard parton scattering. Their spectral functions suffer modifications as a consequence of Debye screening of the heavy-quark potential at finite temperature [3, 4]. One of the most remarkable signatures of this phenomenon is the sequential suppression of quarkonium states, which implies that the suppression of quarkonia is stronger for the states with lower binding energy. Measurements for the sequential suppression have been measured in both charmonium (J/ψ, ψ') [5] and bottomonium ($\Upsilon(nS)$, with n = 1, 2, 3) [6] families at a center-of-mass energy per nucleon pair $\sqrt{s_{\mathrm{NN}}}$ = 2.76 TeV. Recent measurements of Y states at $\sqrt{s_{\mathrm{NN}}}$ = 5.02 TeV by the CMS experiment showed the strong suppression of Y(2S) and Y(3S) states relative to the ground state [7] providing constraints for the theoretical models of the medium. The measurement of individual yields of each Y state as well as their nuclear modification factors, R_{AA}, provide deeper insights in the thermal properties of the medium and are expected to extend our understanding of the nature of color-deconfinement in heavy ion collisions.

We report on the measurement of differential cross sections of Y states decaying to two opposite-sign muons in PbPb and pp collisions. The data were taken by the CMS experiment at $\sqrt{s_{\mathrm{NN}}}$ = 5.02 TeV during the heavy ion run period of November-December 2015. The nuclear modification factors for each Y state, derived from the differential cross sections, are studied as function of the transverse momentum, p_{T}, rapidity, y, and collision centrality.

2 The CMS detector

The central feature of the CMS apparatus is a superconducting solenoid of 6 m internal diameter, providing a magnetic field of 3.8 T. Within the solenoid volume are a silicon tracker, a lead tungstate crystal electromagnetic calorimeter (ECAL), and a brass and scintillator hadron calorimeter (HCAL), each composed of a barrel and two endcap sections. Muons are detected in the pseudorapidity interval $|\eta| < 2.4$ using gas-ionization detectors made of three technologies: drift tubes, cathode strip chambers, and resistive-plate chambers, embedded in the steel flux-return yoke of the solenoid. The silicon tracker is composed of pixel detectors followed by microstrip detectors. The transverse momentum of muons matched to tracks reconstructed in the silicon detector is measured with a resolution better than 1.5% for particles with $p_{\mathrm{T}} = 100\,\mathrm{GeV}/c$ [8]. This high resolution is the result of the 3.8 T magnetic field and the high granularity of the silicon tracker. In addition, CMS has extensive forward calorimetry, including two steel and quartz-fiber Cherenkov hadron forward (HF) calorimeters that cover the range $2.9 < |\eta| < 5.2$. These detectors are used in the present analysis to select events and to determine the centrality of PbPb collisions. A more detailed description of the CMS detector, together with a definition of the coordinate system used and the relevant kinematic variables, can be found in Ref. [9].

3 Data and Monte Carlo samples

The Y mesons are identified using their dimuon decay channel. In both pp and PbPb collisions, the dimuon events are selected by a fast, hardware-based level-1 trigger system which requires

two muon candidates in a given bunch crossing with no explicit limitations on their momentum. In pp collisions, this trigger sampled a luminosity of 28.0 pb^{-1}. The PbPb data consist of two datasets. One used the same trigger algorithm as in pp data, with an additional pre-scale factor, collecting an integrated luminosity of 368 $\mu\mathrm{b}^{-1}$. This trigger is used in this analysis when discussing centrality-integrated results. A second dataset, sampling the integrated luminosity of 464 $\mu\mathrm{b}^{-1}$ by selecting peripheral collisions with no pre-scale, is used to analyze the centrality dependence in the 30–100% centrality range.

Hadronic collisions are selected using information from the HF calorimeter in coincidence with a bunch crossing identified by beam pick-up timing detectors. Events are required to have at least 3 towers in the HF, each with an energy above 3 GeV, on both sides of the interaction point. Moreover, a primary vertex reconstructed with at least two tracks is required. An filter on the compatibility of the silicon pixel cluster width and the vertex position is also applied.

Single muons are selected in the kinematic range $p_{\mathrm{T}}^{\mu} > 4$ GeV/c, $|\eta^{\mu}| < 2.4$. The muon tracks are required to have at least 6 hits in the silicon tracker and one hit in the silicon pixel detector, and to match with at least one segment in any station of the muon system. The muon momentum is derived from a fit to the tracker hits. The distance of the track from the closest primary vertex must be less than 20 cm in the longitudinal direction and 3 mm in the transverse direction. When forming a muon pair, the two muons are required to have opposite charges, to match the dimuon trigger, and to originate from a common vertex with a χ^2 probability larger than 1%. The dimuon kinematic range studied for this analysis is $p_{\mathrm{T}}^{\mu\mu} < 30$ GeV/c and $|y^{\mu\mu}| < 2.4$. Y mesons in this p_{T} range comprise 99% of the total yield.

Monte Carlo (MC) simulated events are used to calculate correction factors for the geometrical acceptance and reconstruction efficiency. The samples are generated using PYTHIA 8.209 [10] for the pp environment and PYTHIA 8.209 embedded in HYDJET for the PbPb case. The CMS detector response is simulated using GEANT4 [11]. The MC samples are reweighted to match the p_{T} distribution found in data.

4 Analysis procedure

4.1 Signal Extraction

The raw yields of Y mesons are extracted using unbinned maximum-likelihood fits to the invariant mass spectra. The signal of each Y state is modeled by a double Crystal Ball (CB) function [12] in order to account for the slightly different resolutions in the barrel region compared to the endcap region of the detector. This is done by allowing the two CB width parameters to vary, whereas the mass and the two radiative-tail parameters are kept the same as these are not affected by resolution. For normalization, one CB parameter sets the overall normalization, i.e. the Y yield, with the second CB normalization parameter chosen to describe the fraction of the total yield described by the second CB function. The mass parameter of the ground state is left free to allow for possible shifts in the absolute momentum calibration of the reconstructed tracks. To describe the excited states, the radiative-tail parameters were constrained to be identical to those of the ground state, while the mass and width parameters were constrained to scale by the ratio of the PDG mass values [13]. The background is modeled with an error function multiplied by an exponential. The background yield, the error function mean and width, and the decay parameter of the exponential are the parameters used to describe the background shape. An alternative background model using a 4^{th} order Chebyshev polynomial is used to estimate systematic uncertainties on the yield extraction.

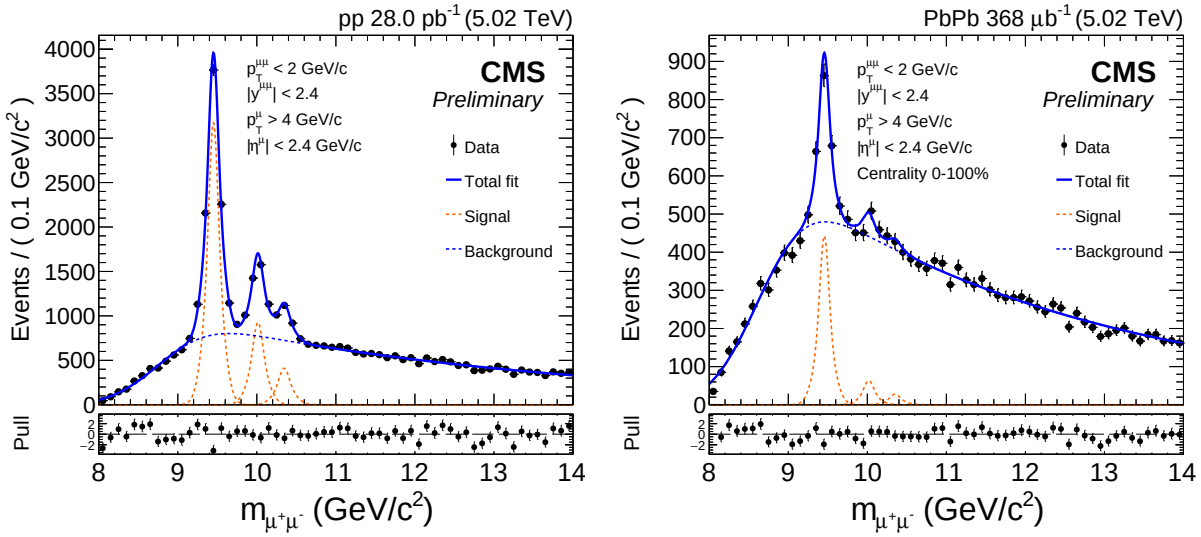

Figure 1: Invariant mass distribution of muon pairs in pp (left) and PbPb (right) collisions, for the kinematic range, $p_{\mathrm{T}}^{\mu\mu} < 2$ GeV/c and $|y^{\mu\mu}| < 2.4$. The result of the fit and the corresponding pull distributions are also shown.

Figure 1 shows the dimuon invariant mass distributions in pp (left) and PbPb (right) collisions for the p_{T} bin of $p_{\mathrm{T}}^{\mu\mu} < 2$ GeV/c and $|y^{\mu\mu}| < 2.4$. The data are well described by the fit model throughout the full kinematic range considered in this analysis.

The Y(3S) is observed to have a very strong suppression in all the PbPb bins analyzed. We therefore obtain 68% and 95% confidence level (CL) upper limits on Y(3S) R_{AA} using the Feldman–Cousins method [14].

4.2 Corrections

To obtain cross sections, the raw yields extracted from the fits to the dimuon invariant mass spectra are corrected for acceptance, efficiency and luminosity. The acceptance, corresponding to the fraction of detectable dimuon events originating from Y mesons within the acceptance cuts of the analysis, is evaluated using MC samples. The acceptance values obtained for the full kinematic region considered are 22%, 28%, and 32% for Y(1S), Y(2S) and Y(3S), respectively. The average dimuon efficiency is determined as the probability that a dimuon pair within the acceptance range is reconstructed offline, satisfies the trigger condition, and passes the analysis quality cuts. The efficiency is also calculated using MC, but we apply scaling factors obtained with the data-driven *tag-and-probe* (T&P) method [15] to compensate for imperfections in the simulation on an event-by-event basis. The average efficiencies for each state, integrated over the full kinematic range, are 79%, 80%, and 80% in PbPb collisions and 2 percentage points higher in case of pp.

The integrated luminosity of 28.0 pb^{-1} is used to normalize the raw yields for pp data. In the case of PbPb data, the number of heavy-ion collision events sampled by the trigger together with the average nuclear overlap function, T_{AA}, are used as normalization. The overlap function T_{AA} is calculated a Glauber monte carlo (MC) simulation [16], and denotes the number of binary nucleus-nucleus (NN) collisions divided by the NN cross section. It is therefore interpreted as the NN-equivalent integrated luminosity per heavy-ion collision.

4.3 Systematic Uncertainties

The following sources of systematic uncertainties are considered: signal yield extraction related to the choice of signal and background models, acceptance and efficiency corrections, and integrated luminosities. The uncertainty from the choice of signal model is estimated by fitting the data using a single CB function in combination with a Gaussian instead of two CBs. The uncertainties are determined by calculating the difference between the yield obtained with the alternative model compared to the nominal one. The differences are in the range of 1–15% for the Y(1S) meson and 1–19% for the Y(2S) meson. The systematic uncertainty due to the choice background model is estimated using two alternative background functions. One is in the form of a 4^{th} order polynomial function and the other is an exponential plus an additional linear function. The differences of yields of these two models compared to the nominal one are added in quadrature and are typically in the range of 0.5–3% for the Y(1S) meson and 1–25% for the Y(2S) meson. The effects of reweighting the p_{T} distribution on the correction factors are also considered as systematic uncertainties. In the case of efficiencies, we also consider uncertainties due to the T&P method and the statistical uncertainty of the scaling factors. The uncertainties add up to less than 2% in case of the efficiency and less than 5% for the acceptance. The global uncertainty on the pp luminosity measurement is 2.3% which is obtained from van der Meer scan taken during the running period [17]. An uncertainty of 2% is quoted for the number of minimum bias (MB) events, N_{MB}, for PbPb collisions, which accounts for the inefficiency of collisional event counting. For the R_{AA} calculation, T_{AA} uncertainties, estimated via varying the Glauber model parameters within their uncertainty, are added in quadrature for each centrality bin.

5 Results

The cross sections and R_{AA} results are measured in several p_{T} and rapidity bins, set to ensure that a reasonable number of events per bin are available for fitting.

$$\begin{aligned} &\text{6 bins for Y(1S) :} && [0,2],\,[2,4],\,[4,6],\,[6,9],\,[9,12],\,[12,30]\ \text{GeV}/c \\ &\text{3 bins for Y(2S) :} && [0,4],\,[4,9],\,[9,30]\ \text{GeV}/c \\ &\text{2 bins for Y(3S) :} && [0,6],\,[6,30]\ \text{GeV}/c \end{aligned} \tag{1}$$

The rapidity bins are evenly divided into six, three and two for Y(1S), Y(2S) and Y(3S), respectively. In order to study the behaviour of the nuclear modification factor as a function of centrality, centrality bin limits for the R_{AA} measurement are chosen as follows: [0, 5, 10, 20, 30, 40, 50, 60, 70, 100%] for Y(1S) and Y(2S) and [0, 30, 100%] for Y(3S).

5.1 Differential cross sections in pp and PbPb collisions

The differential production cross sections of Y mesons decaying in the dimuon channel in pp collisions, $B\frac{\mathrm{d}^2\sigma}{\mathrm{d}p_{\mathrm{T}}\mathrm{d}y}$, where B denotes the branching fraction for the decay $\Upsilon \to \mu^+\mu^-$, are given by

$$B\frac{\mathrm{d}^2\sigma}{\mathrm{d}p_{\mathrm{T}}\mathrm{d}y} = \frac{N_{\Upsilon}/(\mathcal{A}\,\varepsilon)}{\mathcal{L}_{\mathrm{Int}}\Delta p_{\mathrm{T}}\Delta y}\,. \tag{2}$$

The quantity N_{Υ} corresponds to the extracted raw yield of Y mesons in a given (p_{T}, y) bin, $(\mathcal{A}\,\varepsilon)$ represents the average acceptance and efficiency, $\mathcal{L}_{\mathrm{Int}}$ is the integrated luminosity, and Δp_{T} and Δy are the widths of the given $(p_{\mathrm{T}},\ y)$ bin. For PbPb data, $\mathcal{L}_{\mathrm{Int}}$ is replaced by $(N_{\mathrm{MB}} \times T_{\mathrm{AA}})$

as explained in Section 4.2, to compare the pp and PbPb data under the hypothesis of binary-collision scaling.

Figure 2 shows the differential production cross sections of Υ mesons as a function of $p_T^{\mu\mu}$ in pp (left) and PbPb (right) collisions. The data points are placed at the center of each bin. The corresponding results versus $|y^{\mu\mu}|$ are shown in Fig. 3. The Υ(3S) cross sections are presented only for pp collisions because the results in PbPb are statistically consistent with zero for all bins.

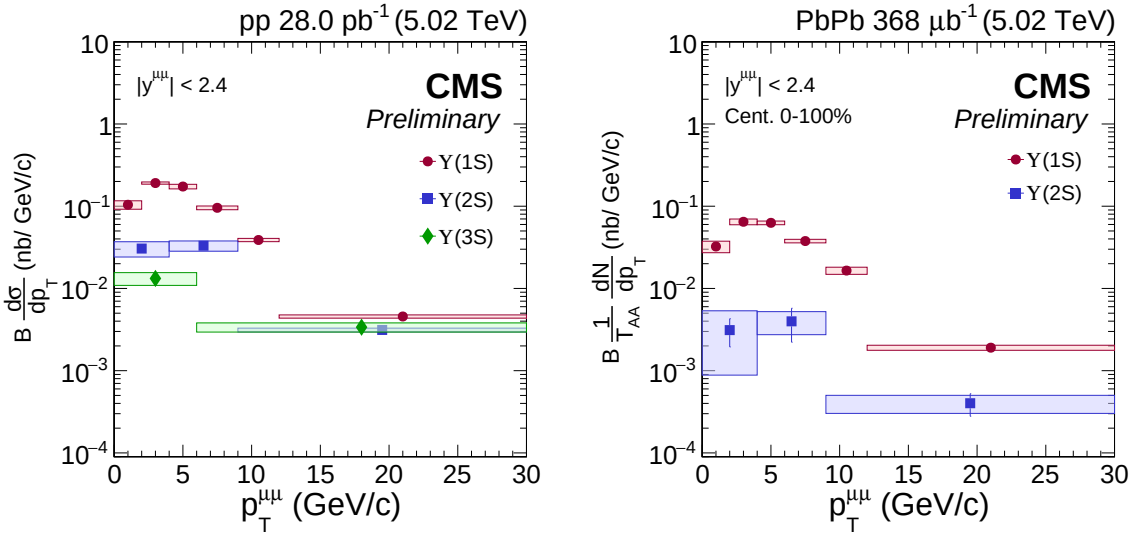

Figure 2: Double differential cross sections of the Υ(1S), Υ(2S), and Υ(3S) mesons as a function of p_T for pp (left) and PbPb (right) collisions. The error bars represent the statistical and the boxes the systematic uncertainties. The global luminosity uncertainties of 2.3% in pp and 2% in PbPb N_{MB} are not shown.

5.2 Nuclear modification factor R_{AA}

The nuclear modification factor is derived from the cross sections given in pp and PbPb by

$$R_{AA}(p_T, y) = \frac{d^2N_\Upsilon^{AA}/dp_T dy}{< T_{AA} > d^2\sigma_\Upsilon^{pp}/dp_T dy} \quad (3)$$

where $< T_{AA} >$ is the average value of T_{AA} computed in each centrality bin.

Figure 4 shows the nuclear modification factor for the Υ(1S), Υ(2S), and Υ(3S) mesons as functions of $p_T^{\mu\mu}$ (left) and $|y^{\mu\mu}|$ (right). The p_T-dependent R_{AA} of the Υ(1S) meson shows a slight increase. The results of Υ(2S) and Υ(3S) states are consistent with being constant with p_T. A flat rapidity dependence is observed for all three states. Hence, the Υ excited states are found to have a large suppression ($R_{AA} < 0.2$) over the full kinematic range explored here. The kinematic dependence of R_{AA} is useful to constrain models of Υ suppression in a deconfined medium [18].

The dependence of R_{AA} on the average N_{part} is depicted in Fig. 5, where N_{part} is defined as the number of nucleons participating in the hadronic interaction in a nucleus-nucleus collision. The average of N_{part} in each centrality bin is estimated using the Glauber MC simulation.

As noted earlier, we observe a very strong suppression of Υ(3S) meson and therefore extract only upper limits at 68% and 95% CL. The nuclear modification factor decreases with centrality

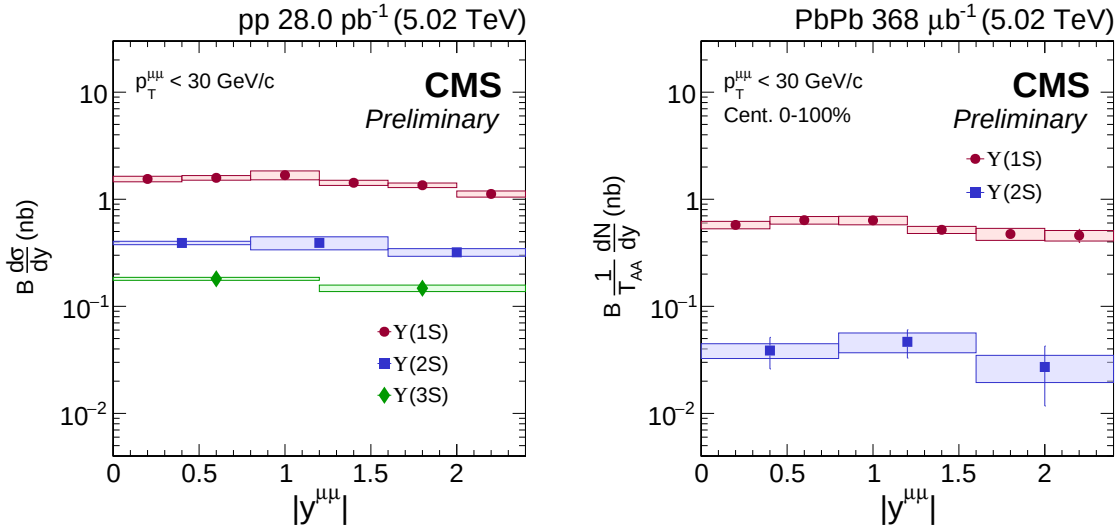

Figure 3: Differential cross sections of the Υ(1S), Υ(2S), and Υ(3S) mesons as a function of rapidity for pp (left) and PbPb (right) collisions. The error bars represent the statistical and the boxes the systematic uncertainties. The global luminosity uncertainties of 2.3% in pp and 2% in PbPb N_{MB} are not shown.

in case of the Υ(1S) and Υ(2S) mesons, a pattern that has already been observed at $\sqrt{s_{\mathrm{NN}}}$ = 2.76 TeV [6].

The R_{AA} of Υ(1S) over the full centrality region is measured to be 0.364 ± 0.014 (stat.) $\pm$ 0.048 (syst.), which is moderately lower than the result at $\sqrt{s_{\mathrm{NN}}}$ = 2.76 TeV ($0.453 \pm 0.014 \pm 0.048$). The centrality-integrated results for the Υ(2S) and Υ(3S) states are statistically consistent with the data at $\sqrt{s_{\mathrm{NN}}}$ = 2.76 TeV. Their values at $\sqrt{s_{\mathrm{NN}}}$ = 5.02 TeV are 0.104 ± 0.021 (stat.) $\pm$ 0.014 (syst.) for Υ(2S) and below 0.071 at 95% CL for Υ(3S). For the Υ(3S) meson, we therefore observe the smallest R_{AA} value of any charged hadron. For comparison, the R_{AA} measured for charged hadrons by CMS at $\sqrt{s_{\mathrm{NN}}}$ = 5.02 TeV reaches values as low as $\approx$ 0.14 for $0-5\%$ most central events at $p_{\mathrm{T}} \approx 7$ GeV [19].

The measured Υ R_{AA} are consistent with theory predictions of Υ suppression in a model where Υ properties are based on lattice heavy-quark potentials, and evolved using anisotropic hydrodynamics. This model indicates that the initial medium temperature increases from $\approx$ 550 MeV at $\sqrt{s_{\mathrm{NN}}}$ = 2.76 TeV to $\approx$ 630 MeV at $\sqrt{s_{\mathrm{NN}}}$ = 5.02 TeV in PbPb collisions [18].

6 Summary

The pp and PbPb data at $\sqrt{s_{\mathrm{NN}}}$ = 5.02 TeV collected with the CMS detector were analyzed to measure the cross sections of Υ(1S), Υ(2S), and Υ(3S) mesons and their nuclear modification factors as functions of p_{T}, $|y|$ and centrality. A gradual decrease of R_{AA} with centrality for the Υ(1S) and Υ(2S) states is observed. We measure a small increase of R_{AA} as function of p_{T} for the Υ(1S) state, while R_{AA} values of the Υ(2S) and Υ(3S) states are consistent with being constant. For all three Υ states we observe a constant rapidity dependence of R_{AA} in the measured region. The modification of Υ(1S) is larger than the one seen at $\sqrt{s_{\mathrm{NN}}}$ = 2.76 TeV, where Υ(1S) mesons were suppressed by factor of $\approx$ 2. This result hints at an increase of the temperature of the medium created by heavy ion collisions at higher collision energy. We observe the nuclear modification factor to be below 0.071 at 95% CL, making this the smallest R_{AA} observed for

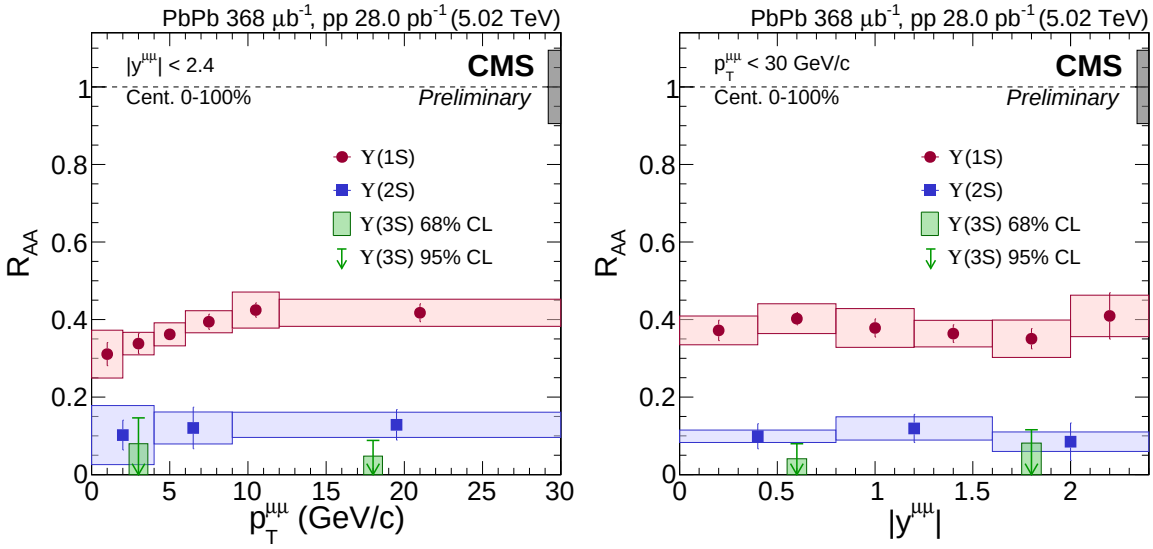

Figure 4: Nuclear modification factors of Υ(1S), Υ(2S) and Υ(3S) meson as functions of p_{T} (left) and rapidity (right). The error bars represent the statistical and the boxes the systematic uncertainties. The gray box near the line at unity displays the global uncertainty which consists of the uncertainties from T_{AA}, pp luminosity and PbPb N_{MB}.

any hadron.

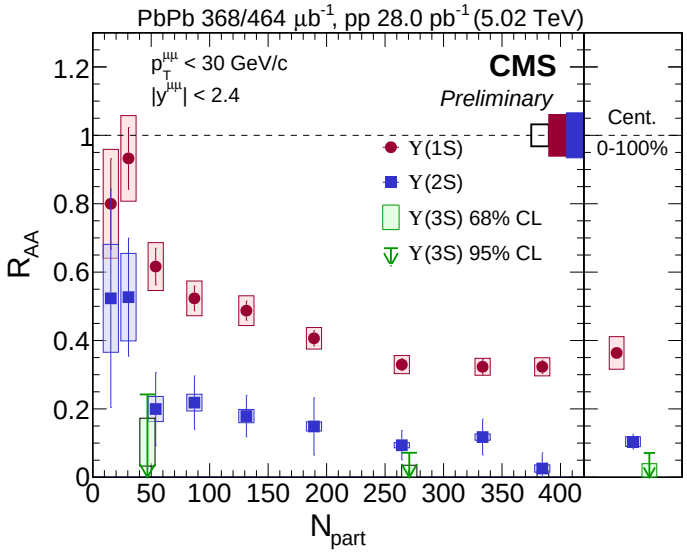

Figure 5: Nuclear modification factors of Y(1S), Y(2S) and Y(3S) mesons as a function of N_{part}. The error bars represent the statistical and the boxes the systematic uncertainties. The black box near the dashed line at unity represents the global uncertainty in pp luminosity and PbPb N_{MB} which applies to both Y(1S) and Y(2S) states. The red and blue boxes show the uncertainties of pp yields for Y(1S) and Y(2S) states, respectively. The global uncertainties for the Y(3S) results are embedded in the upper limit computation. For the centrality-integrated results in the right sub-panel, the systematic uncertainty values include the global uncertainties.

References

[1] F. Karsch and E. Laermann, "Thermodynamics and in-medium hadron properties from lattice QCD", in *Quark-Gluon Plasma III*, R. C. Hwa and X.-N. Wang, eds. World Scientific Publishing Co. Pte. Ltd., 2004. arXiv:hep-lat/0305025.

[2] E. V. Shuryak, "Theory of Hadronic Plasma", *Sov. Phys. JETP* **47** (1978) 212.

[3] T. Matsui and H. Satz, "J/ψ suppression by quark-gluon plasma formation", *Phys. Lett. B* **178** (1986) 416, doi:10.1016/0370-2693(86)91404-8.

[4] S. Digal, P. Petreczky, and H. Satz, "Quarkonium feed down and sequential suppression", *Phys. Rev. D* **64** (2001) 094015, doi:10.1103/PhysRevD.64.094015, arXiv:hep-ph/0106017.

[5] CMS Collaboration, "Suppression and azimuthal anisotropy of prompt and nonprompt J/ψ production in PbPb collisions at $\sqrt{s_{NN}}$ = 2.76 TeV", *Submitted to: Eur. Phys. J. C* (2016) arXiv:1610.00613.

[6] CMS Collaboration, "Suppression of $\Upsilon(1S)$, $\Upsilon(2S)$ and $\Upsilon(3S)$ production in PbPb collisions at $\sqrt{s_{NN}}$ = 2.76 TeV", *Submitted to: Phys. Lett. B* (2016) arXiv:1611.01510.

[7] CMS Collaboration, "Strong suppression of Υ excited states in PbPb collisions at $\sqrt{s_{NN}} = 5.02$ TeV",.

[8] CMS Collaboration, "Measurement of momentum scale and resolution using low-mass resonances and cosmic ray muons", CMS Physics Analysis Summary CMS-PAS-TRK-10-004, 2010.

[9] CMS Collaboration, "The CMS experiment at the CERN LHC", *JINST* **3** (2008) S08004, doi:10.1088/1748-0221/3/08/S08004.

[10] T. Sjöstrand, S. Mrenna, and P. Skands, "PYTHIA 6.4 physics and manual", *JHEP* **05** (2006) 026, doi:10.1088/1126-6708/2006/05/026, arXiv:hep-ph/0603175.

[11] GEANT4 Collaboration, "GEANT4: A Simulation toolkit", *Nucl. Instrum. Meth.* **A506** (2003) 250–303, doi:10.1016/S0168-9002(03)01368-8.

[12] M. J. Oreglia, "A study of the reactions $\psi' \to \gamma\gamma\psi$". PhD thesis, Stanford University, 1980. SLAC Report R-236.

[13] Particle Data Group Collaboration, "Review of Particle Physics", *Chin. Phys. C* **38** (2014) 090001, doi:10.1088/1674-1137/38/9/090001.

[14] G. J. Feldman and R. D. Cousins, "A unified approach to the classical statistical analysis of small signals", *Phys. Rev. D* **57** (1998) 3873, doi:10.1103/PhysRevD.57.3873, arXiv:physics/9711021.

[15] CMS Collaboration, "Measurements of Inclusive W and Z Cross Sections in pp Collisions at $\sqrt{s} = 7$ TeV", *JHEP* **01** (2011) 080, doi:10.1007/JHEP01(2011)080, arXiv:1012.2466.

[16] C. Loizides, J. Nagle, and P. Steinberg, "Improved version of the PHOBOS Glauber Monte Carlo", *SoftwareX* **1-2** (2015) 13, doi:10.1016/j.softx.2015.05.001, arXiv:1408.2549.

[17] CMS Collaboration, "CMS Luminosity Calibration for the pp Reference Run at $\sqrt{s} = 5.02$ TeV", CMS Physics Analysis Summary CMS-PAS-LUM-16-001, 2016.

[18] B. Krouppa and M. Strickland, "Predictions for bottomonia suppression in 5.023 TeV Pb-Pb collisions", *Universe* **2** (2016), no. 3, 16, doi:10.3390/universe2030016, arXiv:1605.03561.

[19] CMS Collaboration, "Charged-particle nuclear modification factors in PbPb and pPb collisions at $\sqrt{s_{\mathrm{NN}}} = 5.02$ TeV", *Submitted to: JHEP* (2016) arXiv:1611.01664.